Geophys. J. Int. (1996) **127,** 595–604

Hydraulic crack propagation in a porous medium

A. C. Fowler and D. R. Scott

Mathematical Institute, Oxford University, 24–29 St Giles', Oxford OX1 3LB, *UK*
Department of Geology, University College, Gower Street, London WC1E 6BT, *UK*

Accepted 1996 July 3. Received 1996 June 24; in original form 1995 March 13

SUMMARY

We develop a model for the propagation of a fluid-filled crack in a porous medium. The problem is motivated by the mechanism whereby drainage networks may form in partially molten rock below the Earth's lithosphere. Other applications include the propagation of hydraulic fractures in jointed rocks and in oil drilling operations, and the formation of dessication cracks in soils. Motivated by the lithospheric problem, we study a situation in which gravity acts in the direction of crack propagation. The model couples the elastohydrodynamic equations of crack propagation with a pore pressure field in the porous rock, which drives the fluid flow which supplies the crack. The effect of the pore flow is to include a diffusional term in the evolution equation for the crack width, thus allowing a crack initiated at the base of the lithosphere to propagate down into the asthenosphere. Asymptotic and numerical solutions are presented for this crack evolution. However, the predicted drainage of melt into this crack is tiny compared with the upward percolative melt migration, and the predicted width of cracks (millimetres) is much too small to allow propagation of melt into the lithosphere without freezing. As a mechanism to explain magma fracturing in the lithosphere, the process described here therefore requires further refinement.

Key words: cracks, magma, poroelasticity.

1 INTRODUCTION

The transport of magma to the surface of the Earth's crust is effected through fissures and dykes, which are initiated as cracks in the lithosphere or crust and then propagate upwards (Spence, Sharp & Turcotte 1987; Lister & Kerr 1991). The propagation is driven by 'magma fracturing', whereby buoyant magma generates the crack pressure head necessary to drive the crack upwards. The fracture toughness of the rock is very small, and the resistance to flow and propagation is primarily due to viscosity.

Many authors have shown that cracks can be propagated through the lithosphere at speeds of the order of metres per second and widths of the order of metres. In some cases (at mid-ocean ridges) fracture is initiated above an axial magma chamber; at mid-plate hot spots such as Hawaii, however, cracks must initiate below the lithosphere, in or just above the region of partially molten rock from which the magma derives. Indeed, Fowler (1985) hypothesized that a porous partially molten rock would be susceptible to fracture under quite small tensile stresses, because of the weakening effects of the pore fluid pressure (much as pore water pressure influences landslides), and there is some evidence of the formation of cracks in exposed ophiolites (Nicolas 1986).

Models of lithospheric crack propagation (e.g. Emerman, Turcotte & Spence 1986) assume a given supply rate from the source region, but, to date, none has provided a coherent account of the mechanism whereby the magma supply is provided. In this paper we provide a first effort to give such an account. While we describe a mechanism that is capable of extracting melt through fractures in the partially molten source region, insofar as it is dynamically consistent, we nevertheless find that it is not viable practically, and some other enhancement of the process is required to provide the melt extraction that occurs.

Magma is thought to originate by pervasive partial melting in the mantle. Experimental observations of the microscopic texture of equilibrated ultramafic partial melts show that both the solid and liquid phases are fully connected (e.g. Vaughan, Kohlstedt & Waff 1982). These observations suggest that the rheology of the porous framework of solid will remain similar to that of a completely solid material, but that magma can percolate through a pervasive network of tubules. The density difference between the magma and solid provides a driving force for the ascent of magma relative to the solid framework. It therefore seems likely that the initial process of magma transport is by pervasive percolative flow.

In a general sense, these two transport mechanisms must 'join up'. One possibility is that the transition always takes place through some kind of 'magma chamber', i.e. a relatively large volume containing only magma. Magma would perhaps be supplied to the base of the chamber by percolation, and leave the chamber in cracks.

There is, however, evidence that cracks operate to transport magma below crustal magma chambers, in the mantle source regions where the magma is produced. Mantle melting beneath the diverging plate takes place in a depth range between approximately 10 and 60 km beneath the sea floor. Because of the thermodynamic properties of the mineral phases present in the parental mantle peridotite, the composition of the magma produced varies significantly through this depth range. The observed systematics of major elements in mid-ocean-ridge basalts (MORBs) (e.g. Klein & Langmuir 1987) indicates that samples of magma throughout the depth range of melting are delivered to the shallow oceanic crust without re-equilibrating with the mineral assemblage at intervening depths.

The physical implication of this geochemical evidence is that the magma must move quickly enough to avoid diffusive re-equilibration. Percolative transport is far too slow to accomplish this, if (as is likely) the dimensions of the channels in the permeable network are related to the grain size of the partially molten rock.

This idea has been developed quantitatively in simplified models of the production and transport of magmas of varying compositions. For example, Iwamori (1993) presented a 1-D model of the development of the distribution of trace elements during melting and magma transport, including both percolative transport and a conceptual model of crack transport. Again, the characteristic of crack transport is that it does not permit chemical re-equilibrium between the magma and the rock it is ascending through. It is shown that the observed range of incompatible trace-element concentrations in residual peridotites can be produced from a single parental bulk composition if crack transport is reasonably efficient.

Studies of secular disequilibrium in the U–Th radioactive decay series place particularly severe constraints on the mechanics of melting and melt transport. Beattie (1993) demonstrated that, deep within the melting column, melt must be produced slowly but must then be transported rapidly to the surface and erupted. Fractures formed within a partial melt might accomplish this process.

Independent, and arguably more direct, evidence for the presence of magma-filled cracks in the partially molten mantle beneath mid-ocean ridges comes from structural studies of ophiolites. For example, Nicolas (1986) argued that vein-like features observed in the mantle section of the Oman ophiolite are relicts from the melting process.

Magma transport in partially molten rock has always been modelled by Darcy's law for flow in a porous medium. However, Fowler (1985) suggested that a more likely drainage route is through an arborescent network of channels, in analogy with comparable networks in subglacial drainage. Such channels would be maintained open (against viscous closure) by melt-back of the channel walls, and would be initiated by crack formation.

However compelling the evidence, the process of magma transport in cracks in regions of partial melting might appear to be mechanically improbable. Cracks are generally thought to be a feature of brittle deformation, but regions that are hot enough to partially melt (well above 1500 K for ultramafic rock types) deform readily by viscous creep. Such geophysical preconceptions may perhaps be allayed by the observation that there exist viscous flows at the Earth's surface, consisting of polycrystalline solids at the melting point and containing several percent partial melt, where fracturing is commonplace. The flows are alpine glaciers, and the cracks are crevasses. Indeed, the internal hydraulic system of a glacier may be an analogue for the magma drainage system in the mantle.

Even when they are hot enough to melt, rocks remain solid in the sense that they can support elastic stresses for at least limited periods of time. The ratio of the dynamic viscosity to the elastic modulus (the Maxwell time) is a measure of the amount of time taken for viscous creep to dissipate elastic stresses; this is probably about a year for partially molten mantle. A process of crack propagation that is fast enough can, therefore, penetrate material that shows ductile behaviour over longer, geological timescales.

In this paper we propose a model in which magma-filled cracks nucleate near the base of the solid lithosphere, and propagate down into the partially molten asthenosphere, as shown in Fig. 1. The downward propagation is rapid enough to produce elastic behaviour in the partial melt region, and the elastic stress field around the crack tip also draws magma from the surroundings into the crack. Sufficient magma is drawn in both to fill the crack as it extends downwards and to supply magma to the upper tip of the crack as it extends upwards into the lithosphere.

The analysis of crack propagation in porous media is also of interest in natural hydraulic fractures in jointed rocks (Renshaw & Harvey 1994) and in hydrofracturing in oil drilling operations (Cleary & Wong 1985; Boone & Ingraffea 1990). The problem has been studied by Ruina (1978) and Huang & Russell (1985a, b). Most of the solution methods are directly

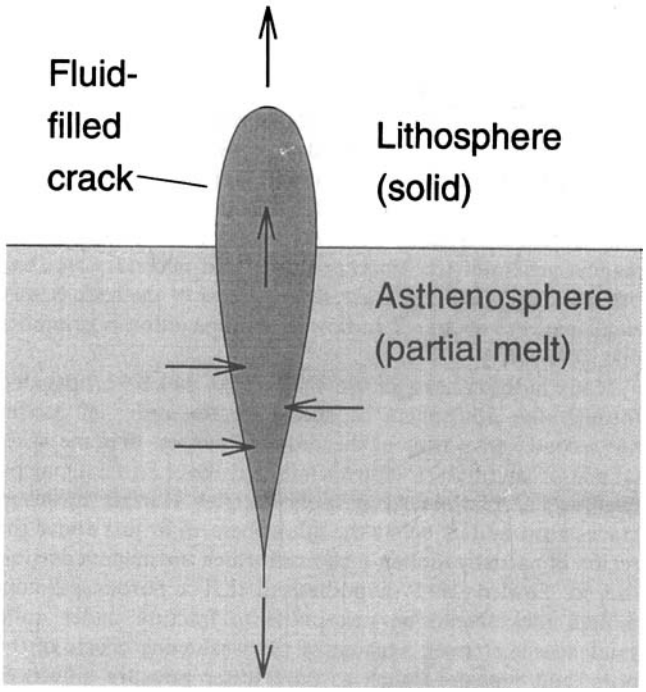

Figure 1. Schematic representation of a crack nucleating at the base of the lithosphere and propagating both upwards and downwards into the asthenosphere.

numerical, and the treatment below seems to extend the model analytically beyond previous work.

Although we achieve our purpose of showing that self-propagation of cracks downwards into an elastic porous medium is dynamically feasible, we also find that, where appropriate parameters that would describe such fracture propagation in the Earth's asthenosphere are used, the resulting crack widths are too small for this mechanism to be a realistic way of extracting magma from source regions.

2 ELASTOHYDRODYNAMIC CRACK MODELLING

We consider a (horizontally) thin vertical crack. We take (x, y) as Cartesian axes, with x pointing vertically downwards, and the crack is situated at $y=0$. We suppose it extends in the z-direction also, but conditions of plane strain are assumed, such that the deformation field is 2-D. We denote the crack width (in the y direction) as $h(x, t)$, and we suppose (or anticipate) that it is of infinite extent in the vertical (the reasons for this are elaborated below).

2.1 Fluid flow

We suppose that the crack is filled with a fluid of density ρ_l and viscosity η. If the crack fluid pressure is p_f, and the crack is thin, then a lubrication approximation can be used to derive a Reynolds' equation relating h and p_f. In the present context, this is

$$\frac{\partial h}{\partial t}+\frac{\partial}{\partial x}\left[\frac{h^3}{12\eta}\left(-\frac{\partial p_f}{\partial x}+\rho_l g\right)\right]=q, \tag{2.1}$$

which is of standard form except that there is a source term q. This is due to the Darcy flow in the porous medium, and we thus take (assuming symmetry across $y=0$)

$$q=\frac{2k}{\eta}\left.\frac{\partial p}{\partial y}\right|_{h+}, \tag{2.2}$$

where k is the permeability of the medium, and p is the pore pressure in the medium.

2.2 Pore pressure determination

The classical theory of poroelasticity due to Biot (1941) supplements linear elasticity equations for a porous elastic solid with a compressibility condition, which leads to a consolidation equation for the pore pressure. In Rice & Cleary's (1976) formulation of Biot's theory, pore pressure is determined by a consolidation-type equation of the form

$$\psi_t=\nabla\cdot[c\nabla\psi], \tag{2.3}$$

where $\psi_t=\partial\psi/\partial t$ and [their second equation (20b)]

$$\psi=\sigma_1+\sigma_2+\frac{3p}{B(1+\nu_u)}, \tag{2.4}$$

where p is the pore pressure, and σ_1 and σ_2 are the normal stresses in conditions of plane strain (i.e. no strain in the x_3-direction). The quantities c, B and ν_u are material properties which represent respectively a consolidation coefficient analogous to that of soil mechanics, a relative compressibility coefficient which relates the change in pore pressure to a corresponding change in confining pressure, and an 'undrained' Poisson's ratio. When the phases are separately essentially incompressible, Rice & Cleary suggest that appropriate values for B and ν_u are

$$B\approx 1, \qquad \nu_u\approx\frac{1}{2}, \tag{2.5}$$

and we shall use these values subsequently. The consolidation coefficient is defined by

$$c=\frac{k}{\eta}\left[\frac{2\mu(1-\nu)B^2(1+\nu_u)^2}{9(1-\nu_u)(\nu_u-\nu)}\right], \tag{2.6}$$

where μ is the shear modulus and ν is the 'drained' Poisson's ratio; in the particular case where B and ν_u are given by (2.5),

$$c\approx\frac{2\mu(1-\nu)k}{(1-2\nu)\eta}. \tag{2.7}$$

In order to compute pore pressure p (and hence the flux q), we require a determination of the elastic stresses.

2.3 Stress distribution and effective stresses

We take σ_1, σ_2 as the normal components of the stress tensor, and τ as the shear stress (thus $\sigma_{11}=\sigma_1$, $\sigma_{22}=\sigma_2$, $\sigma_{12}=\tau$). The stresses satisfy the momentum equations for slow deformations,

$$\frac{\partial\sigma_1}{\partial x}+\frac{\partial\tau}{\partial y}+\rho g=0,$$
$$\frac{\partial\tau}{\partial x}+\frac{\partial\sigma_2}{\partial y}=0, \tag{2.8}$$

where we recall that gravity is assumed to point (downwards) in the positive x-direction. In order to solve these equations, elastic constitutive relations must be posed. In a porous medium such as soil or rock, Terzaghi's principle of effective pressure dictates that the stresses that deform the medium are effective stresses, where the effective normal stresses are

$$\sigma_i'=\sigma_i+\Pi; \tag{2.9}$$

for soils, one often takes $\Pi=p$, in which case the determination of the solid stresses is coupled to the determination of the pore pressure. Skempton (1960) suggests that a more general relationship is

$$\Pi=(1-a)p, \tag{2.10}$$

where a is the specific surface contact area. Thus for soils, $a\approx 0$, but for polycrystalline rocks where the porosity ϕ is small, it may be reasonable to take $a\approx 1$, and thus $\Pi\approx 0$. In this paper, we will indeed assume that $\Pi=0$, so that the solid stresses are determined as for an ordinary elastic solid. This implies that the pore fluid pressure does not affect the deformation of the solid. The merit of this assumption warrants further investigation, however.

2.4 Complex variable formulation

A useful way of writing the solutions of elastic plane strain is in terms of complex variables, and is given by England (1971).

If we denote the strain vector as (u_1, u_2), then

$$2\mu(u_1 + iu_2) = \kappa\Omega - z\overline{\Omega'} - \bar{\omega} - \frac{\mu}{2(\lambda+2\mu)}X,$$

$$\sigma_1 + \sigma_2 = 2\Omega' + 2\overline{\Omega'} - \frac{\lambda+\mu}{\lambda+2\mu}V,$$

$$\sigma_1 - \sigma_2 + 2i\tau = -2z\overline{\Omega''} - 2\overline{\omega'} - \frac{\mu}{\lambda+2\mu}\frac{\partial X}{\partial \bar{z}}, \tag{2.11}$$

where Ω and ω are analytic functions of $z = x + iy$, $\bar{\omega}$ denotes the complex conjugate $\overline{\omega(z)}$, V and X are functions of z and $\bar{z}$, $\kappa = (\lambda + 3\mu)/(\lambda + \mu)$, and λ and μ are the Lamé coefficients. The functions V and X are related to an applied body force (F_1, F_2) per unit mass by

$$\rho(F_1 + iF_2) = \frac{\partial V}{\partial \bar{z}}, \qquad \frac{\partial X}{\partial z} = V, \tag{2.12}$$

where V is chosen to be real. In the present instance, $F_1 = g$ and $F_2 = 0$, thus

$$V = \rho g(z + \bar{z}),$$

$$X = \rho g\left(\frac{1}{2}z^2 + z\bar{z}\right). \tag{2.13}$$

The solution is completed by finding Ω and ω such that the stress satisfies suitable far-field boundary conditions, together with conditions on the crack. If we prescribe a lithostatic pressure $p_0 + \rho g x$ and a tensile stress T as $|y| \to \infty$, then we require

$$\sigma_1 + \sigma_2 = -p_0 - \rho g z + (cc),$$

$$\sigma_1 - \sigma_2 + 2i\tau = -2T, \tag{2.14}$$

as $z \to \infty$, whereas continuity of stress at the crack is ensured by choosing

$$\sigma_2 - i\tau = -p_f \tag{2.15}$$

at $y = 0$. Here, p_f is the crack fluid pressure (no significant shear is exerted on the crack). Note that σ_1 (the vertical stress) is the most compressive stress.

2.5 Reformulation as a Hilbert problem

One can show that

$$\overline{\omega(z)} = \Omega(\bar{z}) - \bar{z}\overline{\Omega'(z)} - \theta(\bar{z}) \tag{2.16}$$

for a function $\theta(z)$ holomorphic outside the crack L. In terms of this, we deduce from (2.11) that

$$\sigma_2 - i\tau = \Omega' + \Omega'(\bar{z}) - (z - \bar{z})\overline{\Omega''} - \theta'(\bar{z})$$
$$+ \frac{1}{2(\lambda+2\mu)}\left[-(\lambda+\mu)V + \mu\frac{\partial X}{\partial \bar{z}}\right], \tag{2.17a}$$

$$2\mu(u_1 + iu_2) = \kappa\Omega - \Omega(\bar{z}) - (\bar{z} - z)\overline{\Omega'} + \theta(\bar{z}) - \frac{\mu}{2(\lambda+2\mu)}X. \tag{2.17b}$$

Satisfaction of the far-field boundary conditions now requires

$$\theta \sim \frac{\mu}{4(\lambda+2\mu)}\rho g z^2 - Tz,$$

$$\Omega' \sim -\frac{1}{2}p_0 - \frac{\mu}{2(\lambda+2\mu)}\rho g z, \qquad z \to \infty. \tag{2.18}$$

To derive a Hilbert problem, we evaluate (2.17a) on both sides $y = 0\pm$ of the crack, and apply (2.15) there. Eliminating θ, we derive the Hilbert problem for Ω', evaluated on $y = 0+$ and $0-$:

$$\Omega'_+ + \Omega'_- = -T - p_f + \frac{\lambda+\mu}{\lambda+2\mu}\rho g x. \tag{2.19}$$

Similarly, using (2.17b), with $[u_1 + iu_2]_-^+ = ih$, where h is the crack width, we find that

$$2i\mu h = (1+\kappa)(\Omega_+ - \Omega_-). \tag{2.20}$$

Finally, we rewrite these relations in terms of μ and the Poisson ratio $\nu = \lambda/[2(\lambda+\mu)]$:

$$\Omega'_+ + \Omega'_- = -T - p_f + \frac{\rho g x}{2(1-\nu)}, \tag{2.21a}$$

$$\Omega_+ - \Omega_- = \frac{i\mu h}{2(1-\nu)}, \tag{2.21b}$$

$$\Omega' \to -\frac{1}{2}p_0 - \frac{1}{4}\left(\frac{1-2\nu}{1-\nu}\right)\rho g z \quad \text{as} \quad z \to \infty. \tag{2.21c}$$

2.6 A singular integral equation for *h*

Solutions of equations of this type have been given, for example by Lister (1990) and Spence *et al.* (1987), in the case of a finite crack. Here, we anticipate an infinite crack on $y = 0$, with $h \to 0$ as $x \to \pm\infty$. The solution of (2.21b) satisfying the boundary condition (2.21c) is

$$\Omega' = -\frac{1}{2}p_0 - \frac{1}{4}\left(\frac{1-2\nu}{1-\nu}\right)\rho g z$$
$$+ \frac{\mu}{2(1-\nu)}\frac{1}{2\pi i}\int_{-\infty}^{\infty} i\frac{\partial h}{\partial s}\frac{ds}{s-z}, \tag{2.22}$$

from which [using (2.22) and (2.21a)]

$$\Omega'_+ + \Omega'_- = -T - p_f + \frac{\rho g x}{2(1-\nu)}$$
$$= -p_0 - \frac{1}{2}\left(\frac{1-2\nu}{1-\nu}\right)\rho g x + \frac{\mu}{2(1-\nu)\pi}\int_{-\infty}^{\infty}\frac{\partial h}{\partial s}\frac{ds}{s-x}, \tag{2.23}$$

thus

$$-p_f + p_0 - T + \rho g x = \frac{\mu}{2(1-\nu)\pi}\int_{-\infty}^{\infty}\frac{\partial h}{\partial s}\frac{ds}{s-x}, \tag{2.24}$$

and this provides the second relation between p_f and h to supplement (2.1). It remains to return to the pore pressure equation to determine the fluid source term q.

2.7 Determination of pore fluid flux

We assume that the consolidation coefficient in (2.3) is constant. Then, since $V_t = \nabla^2 V = 0$ [from (2.13)],

$$\psi_t = c\nabla^2\psi, \tag{2.25}$$

where

$$\psi = 4\,\mathcal{R}e\,\Omega' + \frac{3p}{B(1+\nu_u)}. \tag{2.26}$$

From (2.22),

$$4\,\mathscr{Re}\,\Omega' = \frac{\mu}{(1-\nu)\pi}\mathscr{Re}\int_{-\infty}^{\infty}\frac{\partial h}{\partial s}\frac{ds}{s-z} - 2p_0 - \left(\frac{1-2\nu}{1-\nu}\right)\rho g x, \tag{2.27}$$

and since $\nabla^2\Omega' = 0$, we can finally write (2.25) in the form

$$p_t = c\nabla^2 p - \frac{1}{3}B(1+\nu_u)\frac{\mu}{(1-\nu)\pi}\mathscr{Re}\int_{-\infty}^{\infty}\frac{\partial^2 h}{\partial s\partial t}\frac{ds}{s-z}. \tag{2.28}$$

We suppose, for the moment, that the far-field pore pressure satisfies

$$p \to p_0 - T + \rho g x \quad \text{as} \quad y \to \pm\infty, \tag{2.29}$$

which implies that the pore pressure equals the least compressive stress. It was suggested by Fowler (1985) that a criterion such as this would cause initiation of fracturing near the top of the partial melt region, and (2.29) corresponds to the maintenance of this marginal condition in the far field. The implications of continued over-pressuring are examined further below.

We define P on $y=0$ by prescribing

$$p = p_f = p_0 - T + \rho g x + P \tag{2.30}$$

there. We then define Ψ by

$$p = p_0 - T + \rho g x - \frac{1}{3}B(1+\nu_u)\frac{\mu}{(1-\nu)\pi}\mathscr{Re}\int_{-\infty}^{\infty}\frac{\partial h}{\partial s}\frac{ds}{s-z} + \Psi; \tag{2.31}$$

it follows that

$$\Psi_t = c\nabla^2\Psi,$$

$$\Psi \to 0 \quad \text{as} \quad y \to \pm\infty, \tag{2.32}$$

and with [from (2.24)]

$$P = -\frac{\mu}{2(1-\nu)\pi}⨍\frac{\partial h}{\partial s}\frac{ds}{s-x}, \tag{2.33}$$

it follows that, on $y = 0+$,

$$\Psi = \left[1 - \frac{2}{3}B(1+\nu_u)\right]P. \tag{2.34}$$

If we now adopt the values in (2.5) suggested for incompressible phasic constituents, then (2.34) becomes simply $\Psi \approx 0$ on $y=0+$, whence $\Psi = 0$ everywhere, and the pore pressure is simply given by (2.31) with $\Psi = 0$. In particular, we find that the pore fluid source is

$$q = \frac{2k}{\eta}\frac{\partial p}{\partial y}\bigg|_{0+} = -\frac{4k}{\eta}\mathscr{Im}\frac{\partial p}{\partial z}\bigg|_{y=0} = \frac{\mu k}{\eta(1-\nu)}\frac{\partial^2 h}{\partial x^2}. \tag{2.35}$$

This completes the derivation of the model equation for h.

2.8 Summary

Eq. (2.1) can be written as

$$\frac{\partial h}{\partial t} + \frac{\partial}{\partial x}\left[\frac{h^3}{12\eta}\left(-(\rho-\rho_l)g - \frac{\partial P}{\partial x}\right)\right] = q, \tag{2.36}$$

(2.33) is

$$P = -\frac{\mu}{2(1-\nu)\pi}⨍\frac{\partial h}{\partial s}\frac{ds}{s-x}, \tag{2.37}$$

and the poroelastohydrodynamic equation for h is then [with (2.35)]

$$\frac{\partial h}{\partial t} + \frac{\partial}{\partial x}\left[\frac{h^3}{12\eta}\left\{-(\rho-\rho_l)g - \frac{\partial P}{\partial x}\right\}\right] = \frac{\mu k}{(1-\nu)\eta}\frac{\partial^2 h}{\partial x^2}, \tag{2.38}$$

and the porous flow introduces a diffusive term to the equation. The diffusion coefficient has the form of a coefficient of consolidation, that is, elastic modulus times permeability divided by liquid viscosity. It is because of this that we assumed an infinite crack in the first place. In fact, the derivation of q assuming a finite crack leads to exactly the same expression for q (and thus a contradiction, since the diffusion precludes h reaching zero in a finite distance). Because of the diffusive nature of the flux to the crack, a crack tip does not formally exist, and there is no need to apply a fracture toughness criterion at the tip, as would be the case for a finite crack.

Although it is inviting to think of the fluid-filled crack as a response to the far-field extensional stress T, this quantity does not appear in the final equation (2.38) nor in its boundary conditions. The elastic stresses that deflect porous flow of melt into the crack are in fact perturbations to the far-field stress, set up by the opening and extension of the crack. The only role that T might play would be at the crack tip, favouring crack propagation in the vertical direction.

We see that the diffusive timescale for lengths of order l is $t \sim \eta l^2/\mu k$, while the consolidation timescale for (2.5) is $t \sim l^2/c$. The ratio is thus $\eta c/\mu k$ (=crack diffusion time/Darcy time), so that if this is large, then the pore pressure relaxes more rapidly than the crack.

What if c is not constant? In particular, we study below the situation where a crack also propagates upwards into the (impermeable) lithosphere where $c=0$. However, providing c decreases to zero over a long space-scale, then $\nabla\cdot[c\nabla\psi] \approx c\nabla^2\psi$, and the reasoning above still applies at leading order. Since, in fact, our analysis is concerned with such long scales, this is a reasonable assumption. We can then approximate (2.32) by

$$\Psi_t = c\Psi_{yy}, \tag{2.39}$$

and the solution can be written as a convolution. We do not pursue such issues here.

If, instead of (2.29), an overpressure p_{ex} is applied at $y = \pm\infty$, then Ψ satisfies

$$\Psi_t = c\nabla^2\Psi,$$

$$\Psi \to p_{ex} \quad \text{as} \quad y \to \pm\infty,$$

$$\Psi = 0 \quad \text{on} \quad y = 0 \tag{2.40}$$

[from (2.34), with $B=1$, $\nu_u = 1/2$]. The long time solution of this problem has $\Psi \to 0$ for fixed x, y, the implication of which is that the overpressure can effectively be taken to be zero, since we find below that the relevant timescale of the process is indeed 'large'.

3 ANALYSIS

First, we non-dimensionalize the equations. We can choose distinguished scales $[x]$, $[t]$, $[h]$ and $[P]$ for x, t, h and P which make all the coefficients equal to one. Specifically, we choose

$$[x]=(3k)^{1/5}\left[\frac{\mu}{g\Delta\rho(1-\nu)}\right]^{3/5},$$

$$[h]=\frac{2(1-\nu)}{\mu}g\Delta\rho[x]^2,$$

$$[t]=\frac{12\eta[x]}{[h]^2 g\Delta\rho},$$

$$[P]=g\Delta\rho[x], \tag{3.1}$$

where $\Delta\rho=\rho-\rho_l$, and then the dimensionless equations (2.37) and (2.38) are

$$P=-\frac{1}{\pi}\int\frac{\partial h}{\partial s}\frac{ds}{s-x}, \tag{3.2a}$$

$$h_t+\frac{\partial}{\partial x}\left[h^3\left(-1-\frac{\partial P}{\partial x}\right)\right]=h_{xx}. \tag{3.2b}$$

Using values (Spence *et al.* 1987) of $\mu\sim 2\times10^{10}$ Pa, $\Delta\rho\sim 300$ kg m^{-3}, $g\sim 10$ m s^{-2}, $\nu\approx 1/4$, $\eta\sim 10$ Pa s, $k\sim 10^{-12}$ m^2, we find

$$[x]\sim 73\ \text{m},\qquad [h]\sim 1.2\ \text{mm},\qquad [t]\sim 2\times10^6\ \text{s (23 days)},$$
$$[P]\sim 2.2\times10^5\ \text{Pa (2.2 bars)}. \tag{3.3}$$

These scales have as yet no intrinsic meaning; they simply indicate when all the terms balance.

3.1 An approximate analytic approach

There are conceptual problems with models of crack propagation through the lithosphere. Usually the supply rate of magma to the crack is prescribed, but the way in which this can be done is not clear. In the present context, eqs (3.2) apply without change in the lithosphere, except that the diffusive term is absent. This means that there can be net growth of an upward-propagating crack (in $x<0$), while the crack extends downwards (in $x>0$), and there is net drainage from the source region (corresponding to $h_x<0$ at $x=0$). However, an initial perturbation is necessary to initiate crack propagation. We will give an approximate description of the evolution of an initial perturbation, and give asymptotic estimates for crack length, width and propagation speed. We begin by considering the upward-propagating part of the crack.

3.2 Lithosphere fracture

The model (3.2) applies also for fractures propagating upwards in the lithosphere, providing the diffusion term is removed, since the lithosphere is impermeable. In this case, the upward-propagating crack has a moving tip, whose shape is determined by the fracture toughness. For large cracks ($-x\gg 1$), the term in $\partial P/\partial x$ is small (providing $h\ll x^2$), which implies that the bulbous tip of the crack occupies a small region, and the solution is shock-like. We put $\xi=-x$; it follows that, approximately,

$$h_t+3h^2h_\xi=0, \tag{3.4}$$

and if $h=h_0(t)$ at $x=0$ (with $h=0$ at $t=0$ in $\xi>0$), then $h=0$ for $\xi>x_f(t)$, the crack tip position, and

$$h=h_0\left(t-\frac{\xi}{3h^2}\right)\quad\text{for}\quad 0<\xi<x_f, \tag{3.5}$$

where h_0 is a function of the expression in brackets. The position of the crack tip is then given by $\dot{x}_f=h^2|_{x_f}$, that is

$$\dot{x}_f=h_0(t-x_f/3\dot{x}_f)^2. \tag{3.6}$$

Possibly a more realistic scenario is where a finite amount of fluid is released at $\xi=0$. In this case the blob moves and spreads out behind a front at $\xi_f\sim t^{1/3}$, but continual injection from $x>0$ eventually leads to the same solution as above. Note that if $h_0=bt^{-\beta}$, then

$$x_f=\frac{b}{(1-2\beta)^{1-2\beta}}\left(\frac{3}{2-3\beta}\right)^{2\beta}t^{1-2\beta}, \tag{3.7}$$

providing $\beta<1/3$.

At the front of the crack there is apparently a discontinuity. In reality there is a relatively short zone, where $\partial P/\partial x\sim O(1)$, and h changes rapidly to zero, with $h\sim\delta(x_f-\xi)^{1/2}$ as $\xi\to x_f$ and

$$\delta=\frac{\sqrt{2}K_c}{g\Delta\rho[x]^{3/2}}, \tag{3.8}$$

where K_c is the fracture toughness of the rock (Spence *et al.* 1987). Using values of $K_c=10$ MN m$^{-3/2}$ (Spence *et al.* 1987), $g=10$ m s^{-2}, $\Delta\rho=300$ kg m^{-3}, $[x]=73$ m, we have $\delta\sim 7.5$.

3.3 Asthenospheric fracture

Now let us consider the model equations (3.2) below the origin, in $x>0$. Prescription of $h=h_0$ at $x=0$ will cause h to diffuse downwards, but this is counteracted by the upward advective effect of the flux term $-(h^3)_x$. In the absence of the singular integral term, we can then expect h to relax to a steady state. Regarding the meaning of the singular integral, note that $(s-x)^{-1}$ is crudely representative of $-\delta'(s-x)$ (the derivative of the delta function in the sense of generalized functions), so that (crudely)

$$P\sim\int\frac{\partial h}{\partial s}\delta'(s-x)\,dx=-\frac{\partial^2 h}{\partial x^2}, \tag{3.9}$$

and $-\partial/\partial x[h^3\partial P/\partial x]$ is thus a non-linear long-range diffusive term, which also acts to damp out disturbances. This is confirmed by the Fourier transform of P (see below). The diffusive term and the singular integral may thus be considered to have similar effects.

If the crack propagates downwards over a long time, so that $h\ll x^2$, then we can ignore the integral, so that

$$h_t-\frac{\partial}{\partial x}(h^3)=h_{xx}, \tag{3.10}$$

with

$$h=h_0(t)\quad\text{on}\quad x=0,\qquad h\to 0\quad\text{as}\quad x\to\infty. \tag{3.11}$$

We now have two approximations of h, in $x<0$ and $x>0$, in terms of $h_0(t)=h(0,t)$, which is as yet unknown. Despite the absence of the diffusive term in $x<0$, we require h_x to be continuous at $x=0$, in order that the stresses be continuous.

Eq. (3.10) has a similarity solution $h=t^{-1/4}F(\eta)$, $\eta=x/t^{1/2}$, whence there follows

$$F''+\left(3F^2+\frac{1}{2}\eta\right)F'+\frac{1}{4}F=0. \tag{3.12}$$

With $F_0=F(0)$, we require $h_0=F_0/t^{1/4}$, $h_0'=-F_0/4t^{5/4}$, and $h_x=F'(0)/t^{3/4}$. From (3.4) (with h_x continuous at $x=0$),

$$h_x=h_t/3h^2=h_0'/3h_0^2=-(F_0/4t^{5/4})(t^{1/2}/3F_0^2)=-1/(12F_0t^{3/4});$$

thus appropriate boundary conditions for (3.12) are

$$12F(0)F'(0)+1=0,$$

$$F(\infty)=0. \tag{3.13}$$

The conditions in (3.13) are not sufficient to solve (3.12), however, since by inspection $F\to 0$ as $\eta\to\infty$ automatically (the equation for F is that of a non-linearly damped oscillator). In fact, as $\eta\to\infty$, two independent asymptotic behaviours for F are possible:

$$F_1\sim\frac{1}{\eta}\exp(-\eta^2/4),\qquad F_2\sim\eta^{-1/2}, \tag{3.14}$$

and the general solution will be $F\sim AF_1+BF_2$. If the initial data are of compact support, however, then we expect that the algebraic decay like F_2 will be suppressed, so that the second condition in (3.13) will be strengthened to

$$\eta^{1/2}F\to 0\quad\text{as}\quad\eta\to\infty. \tag{3.15}$$

[This is analogous to the behaviour of the Fisher equation, to which (3.10) is similar: see Murray (1979) for details.] Alternatively, we can note that F_2 would require an infinite volume of magma to be present initially. Solution of (3.12) is then simply done by shooting with various values of F_0, and evaluating $\eta^{1/2}F|_{\eta=L}$ for some large, fixed L. The value of F_0 that is a zero of $\eta^{1/2}F|_L$ can be determined by usual root-finding methods, such as interval bisection.

The appropriate solutions for h_0 and h in $x<0$ are then

$$h_0\sim F_0t^{-1/4}, \tag{3.16}$$

$$h=\frac{1}{\sqrt{6}t^{1/4}}\{(\xi/t^{1/2})+[36F_0^4+(\xi/t^{1/2})^2]^{1/2}\}^{1/2}, \tag{3.17}$$

(and $h\sim t^{-1/4}$ for $\xi\sim t^{1/2}$ as before), and

$$x_f=2\sqrt{3}F_0^2t^{1/2}. \tag{3.18}$$

Computation of the solution of (3.12) and (3.13) yields $F_0=0.4142$ (see Fig. 2), and thus $h_0\sim 0.414t^{-1/4}$, $x_f\sim 0.59t^{1/2}$. We can also compute the tip width at x_f, $h_f\sim 0.54t^{-1/4}$, and the total crack volume, $V\sim 0.8t^{1/4}$.

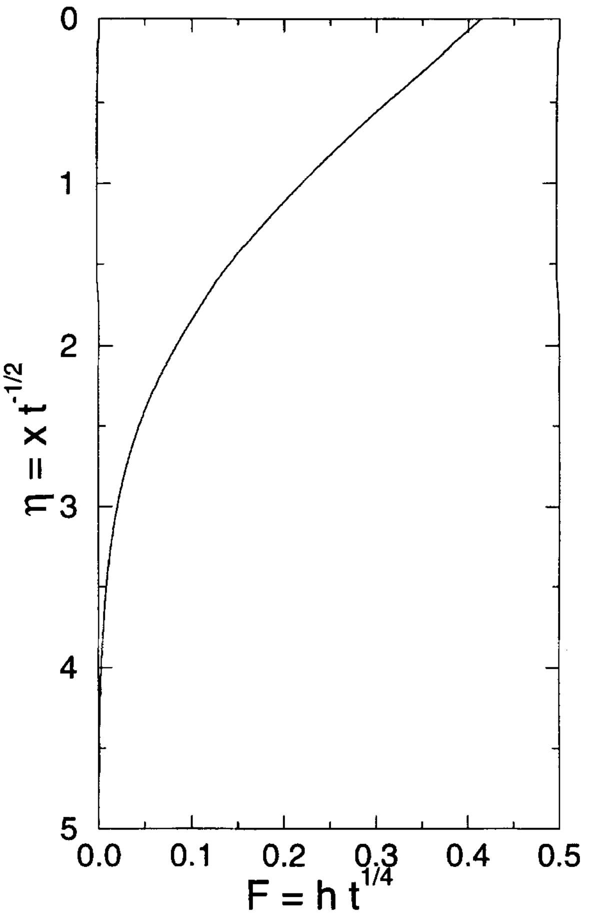

Figure 2. Numerical solution of (3.12) subject to the conditions (3.13) and (3.15). This is an asymptotic solution for the crack profile as a function of depth into the asthenosphere.

3.4 Numerical solution

We have solved the coupled set of equations in (3.2) numerically. First, we note that the singular integral for P in (3.2a) can be evaluated using a spectral method. If $\hat{g}$ denotes the Fourier transform of g, then

$$\begin{aligned}\widehat{H(g)}&=\frac{1}{\pi}\int_{-\infty}^{\infty}e^{ikx}\,dx\,⨍_{-\infty}^{\infty}\frac{g(s)\,ds}{s-x}\\&=-\frac{1}{\pi}\int_{-\infty}^{\infty}g(s)\,e^{iks}\,ds\,⨍_{-\infty}^{\infty}\frac{e^{ik(x-s)}\,dx}{x-s}\\&=-\frac{i}{\pi}\hat{g}\int_{-\infty}^{\infty}\frac{\sin ku\,du}{u}\\&=-i\,\mathrm{sgn}(k)\hat{g}\end{aligned} \tag{3.19}$$

(for real k), where $H(g)$ is the Hilbert transform, and the interchange of the order of integration is justified by the Poincaré–Bertrand formula. Since $\hat{h}_x=-ik\hat{h}$, we have that

$$\hat{P}=-\widehat{H(h_x)}=i\,\mathrm{sgn}(k)\hat{h}_x=|k|\hat{h}. \tag{3.20}$$

The advective derivative in (3.2) is expanded to give

$$h_t=3h^2\left(1+\frac{\partial P}{\partial x}\right)\frac{\partial h}{\partial x}+h^3\frac{\partial^2 P}{\partial x^2}+K(x)\frac{\partial^2 h}{\partial x^2}. \tag{3.21}$$

P is evaluated using (3.20) and fast Fourier transforms. The spatial derivatives of h and P in eq. (3.21) are then evaluated using explicit finite differences. The Two-Step Lax–Wendroff method (Press *et al.* 1992) is used to advance h in time with second-order accuracy.

The non-dimensional permeability function $K(x)$ is used to distinguish between the lithosphere and asthenosphere in the spatial domain of the numerical solution. In the asthenosphere (positive x), $K=1$; in the lithosphere (negative x), $K=K_0\ll 1$ (there is a narrow transition region centred at $x=0$). The small lithospheric permeability K_0 is needed to stabilize the advection of the ascending crack tip. By comparing the advective and diffusive terms in (3.2), the minimum value required is estimated to be

$$K_0=3h_{\max}^2\Delta x, \tag{3.22}$$

where $h_{\max}$ is the maximum crack width and Δx is the spatial grid size. In the numerical procedure K_0 is adapted, as $h_{\max}$ changes, to the minimum value given by eq. (3.22). Note that if $h_{\max} \sim 1$ then $\Delta x \ll 1$ is required in order to permit $K_0 \ll 1$.

The maximum time step permitted, Δt, is usually determined by the diffusive term in the asthenospheric ($K = 1$) part of the spatial domain:

$$\Delta t < 0.2 \Delta x^2 . \tag{3.23}$$

(The numerical factor is empirical.) For the examples shown in Figs 3 and 4, the following parameter choices were used: $\Delta x = 0.1$, $\Delta t = 0.001$. In the initial state, $h_{\max} = 0.3$ and therefore $K_0 = 0.03$. The maximum crack width monotonically decreases, so the lithospheric permeability K_0 is less than one per cent of the asthenospheric permeability during most of the calculation. The example shown used 2048 grid points in x and 10^6 time steps, and took about one day to produce on a Sun SPARC station 10/41. We see that the similarity solution accurately represents the numerical solutions.

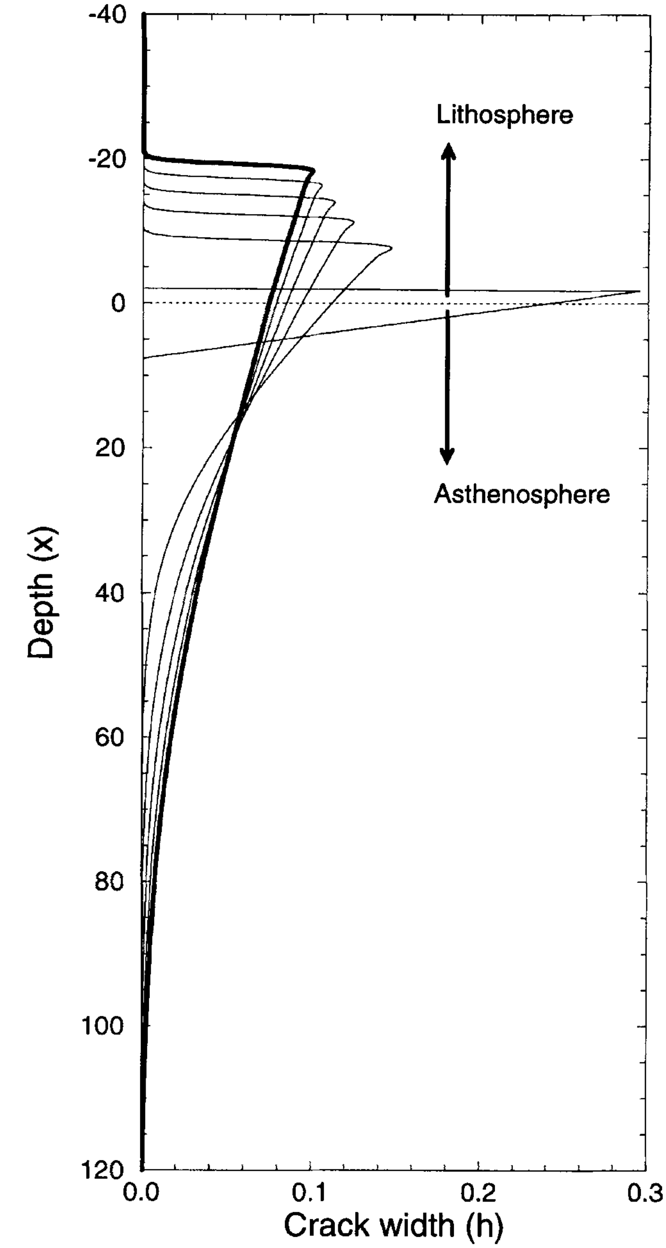

Figure 3. A numerical solution to eq. (3.21), showing the evolution of the crack shape with time. Negative values of the depth coordinate x lie in the solid lithosphere; positive values of x lie in the permeable, partially molten asthenosphere. In the initial state, the crack has a maximum width of approximately 0.3 and is localized to the region around $x = 0$ (the lithosphere–asthenosphere boundary). The other outlines of the crack shape are spaced by time intervals of 200; the final shape, after a time interval of 1000, is shown by a thicker line. The variables are given in terms of units $[h] = 1.2$ mm (for h); $[t] = 2 \times 10^6$ s (for t); $[x] = 73$ m (for h). Thus the final maximum crack width is ≈ 0.1 mm, at a time $\approx 2 \times 10^9$ s ~ 70 years, and extends over a distance ≈ 7 km.

4 CONCLUSIONS

In this paper, we have addressed the issue of explaining how cracks can propagate sub-critically in porous elastic solids, when the crack growth is limited by fluid supply through the porous matrix. Two immediate applications are to joint propagation in wet, porous rocks, and the supposed propagation of magma-bearing fractures downwards into the lithosphere. We focus in particular on this latter problem, with the aim of understanding how an upward-propagating lithospheric crack can tap its supply source in the asthenosphere. In previous studies, the magma supply has always been prescribed as a boundary condition.

In the physically realistic case where the separate phases are incompressible, but the porous mixture is elastically compressible, we show that the fluid supply from the matrix is determined by a diffusive term. This allows the possibility that fractures can propagate in a direction opposite to that of the fluid buoyancy, and, by explicit calculation, we show that lithospheric fractures can propagate upwards while drawing their melt from the porous source region by a downward-propagating asthenospheric crack.

Two issues arise in considering the relevance of our results to asthenospheric melt transport. First, the cracks still require a nucleus from which to grow. Our mechanism allows this point of nucleation to be moved from deep within the region of partial melting to the upper boundary of this region, i.e. to the base of the lithosphere. We argue that it is more likely that cracks nucleate by brittle processes at the base of the lithosphere than it is that they nucleate by some purely viscous process within the asthenosphere (e.g. Stevenson 1989).

Second, the dimensional scales in eq. (3.3) translate our non-dimensional solutions into cracks with speeds of metres per day and widths of millimetres. In the lithosphere such cracks will simply freeze, although the propagation down into the asthenosphere should still be viable. We speculate that the cracks might branch out to form arborescent networks analogous to river drainage networks, supplying a larger and faster single crack in the lithosphere. Alternatively, crack enlargement may arise from the fact that melting in the asthenosphere is due to adiabatic decompression of ascending material. As the fluid flux through the crack increases, the transport of sensible heat with the fluid increases, and local 'melt-back' of the crack walls may occur. A similar process

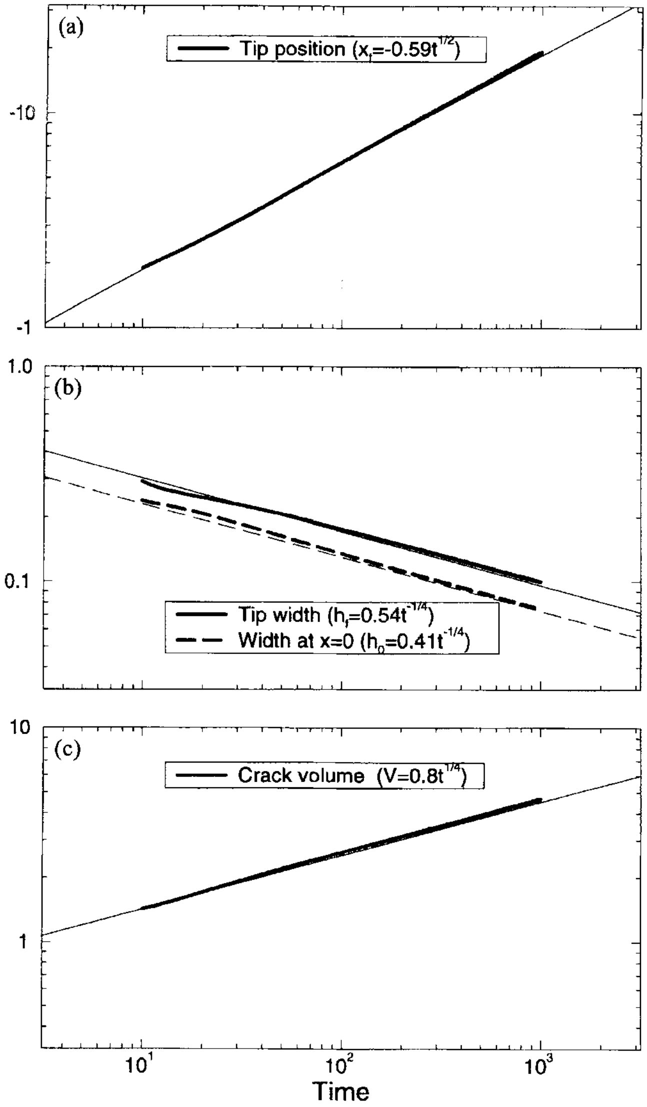

Figure 4. A comparison between the numerical solution shown in Fig. 3, and the asymptotic solutions given in the text and shown in Fig. 2. In all three plots, results from the numerical solution are shown as thicker lines, and the asymptotic forms (given in the legends) are shown as finer lines. In (a) the position of the crack tip is defined as the point at which the crack width drops to half of its present maximum value. In (b) the tip width is the maximum crack width. In (c) the crack volume is, strictly speaking, the area of a vertical section through the crack. The initial crack shape for the numerical solution (shown in Fig. 3) was designed to provide a close match to the asymptotic solution at $t = 10$. The subsequent evolution of the numerical solution closely matches the asymptotic forms.

has been discussed recently in the context of an instability of partial melts in the absence of cracks (Keleman *et al.* 1995; Aharanov *et al.* 1995). In other situations, this mechanism (or a similar one) is known as reaction infiltration instability (Ortoleva *et al.* 1987; Hinch & Bhatt 1990). Our analysis is confined to mechanics, but it is clearly amenable to extensions that incorporate the thermodynamics of melting.

Despite the quantitative uncertainties outlined above, the importance of the work presented here lies in identifying a mechanism by which cracks can participate in melt transport at depth without a requirement that cracks nucleate at depth.

ACKNOWLEDGMENT

David Scott acknowledges the award of a NERC research fellowship.

REFERENCES

Aharonov, E., Whitehead, J.A., Keleman, P.B. & Spiegelman, M., 1995. Channeling instability of upwelling melt in the mantle, *J. geophys. Res.*, **100,** 20 433–20 450.

Beattie, P., 1993. Uranium–thorium disequilibria and partitioning on melting of garnet peridotite, *Nature,* **363,** 63–65.

Biot, M.A., 1941. General theory of three-dimensional consolidation, *J. appl. Phys.*, **12,** 155–164.

Boone, T.J. & Ingraffea, A.R., 1990. A numerical procedure for simulation of hydraulically-driven fracture propagation in poroelastic media, *Int. J. Numer. Anal. Math. Geomech.*, **14,** 27–47.

Cleary, M.P. & Wong, S.K., 1985. Numerical simulation of unsteady fluid flow and propagation of a circular hydraulic fracture, *Int. J. Numer. Anal. Math. Geomech.*, **9,** 1–14.

Emerman, S.H., Turcotte, D.L. & Spence, D.A., 1986. Transport of magma and hydrothermal solutions by laminar and turbulent fluid fracture, *Phys. Earth planet. Inter.*, **44,** 249–259.

England, A.H., 1971. *Complex Variable Methods in Elasticity,* John Wiley.

Fowler, A.C., 1985. A mathematical model of magma transport in the asthenosphere, *Geophys. Astrophys. Fluid Dyn.*, **33,** 63–96.

Hinch, E.J. & Bhatt, B.S., 1990. Stability of an acid front moving through porous rock, *J. Fluid Mech.*, **212,** 279–288.

Huang, N.C. & Russell, S.G., 1985a. Hydraulic fracturing of a saturated porous medium. I: general theory, *Theoret. appl. fract. Mech.*, **4,** 201–213.

Huang, N.C. & Russell, S.G., 1985b. Hydraulic fracturing of a saturated porous medium. II: special cases, *Theoret. appl. fract. Mech.*, **4,** 215–222.

Iwamori, I., 1993. A model for disequilibrium mantle melting incorporating melt transport by porous and channel flows, *Nature,* **366,** 734–737.

Keleman, P.B., Whitehead, J.A., Aharonov, E. & Jordahl, K.A., 1995. Experiments on flow focussing in soluble porous media, with applications to melt extraction from the mantle, *J. geophys. Res.*, **100,** 475–496.

Klein, E.M. & Langmuir, D.H., 1987. Global correlations of ocean ridge basalt chemistry with axial depth and crustal thickness, *J. geophys. Res.*, **92,** 8089–8115.

Lister, J.R., 1990. Buoyancy-driven fluid fracture: similarity solutions for the horizontal and vertical propagation of fluid-filled cracks, *J. Fluid Mech.*, **127,** 213–239.

Lister, J.A. & Kerr, R.C., 1991. Fluid-mechanical models of crack propagation and their application to magma transport in dikes, *J. geophys. Res.*, **96,** 10 049–10 077.

Murray, J.D., 1989. *Mathematical Biology,* Springer-Verlag, Berlin.

Nicolas, A., 1986. A melt extraction model based on structural studies in mantle peridotites, *J. Petrol.*, **27,** 999–1022.

Ortoleva, P., Chadam, J., Merino, E. & Sen, A., 1987. Geochemical self-organisation II: the reactive-infiltration instability, *Am. J. Sci.*, **287,** 1008–1040.

Press, W.H., Teukolsky, S.A., Vettering, W.T. & Flannery, B.P., 1992. *Numerical Recipes,* Cambridge University Press, Cambridge.

Renshaw, C.E. & Harvey, C.F., 1994. Propagation velocity of a natural hydraulic fracture in a poroelastic medium, *J. geophys. Res.*, **99,** 21 667–21 677.

Rice, J.R. & Cleary, M.P., 1976. Some basic stress diffusion solutions for fluid-saturated elastic porous media with compressible constituents, *Rev. Geophys. Space Phys.*, **14**, 227–241.

Ruina, A., 1978. Influence of coupled deformation—diffusion effects on the retardation of hydraulic fracture, in *Proc. 19th US Rock Mech. Symp.*, pp. 274–282, University of Nevada Press, Reno, Nevada.

Skempton, A.W., 1960. Effective stress in soils, concrete and rocks, in *Proc. Conf. Pore Pressure and Suction in Soils*, pp. 4–16, Butterworths, London.

Spence, D.A., Sharp, P.W. & Turcotte, D.L., 1987. Buoyancy-driven crack propagation: a mechanism for magma migration, *J. Fluid Mech.*, **174**, 135–153.

Stevenson, D.J., 1982. Migration of fluid-filled cracks: applications to terrestrial and icy bodies, in *Proc. 13th Lunar Planet. Sci. Conf., AGU*, pp. 768–769, Washington, DC.

Stevenson, D.J., 1989. Spontaneous small-scale melt segregation in partial melts undergoing deformation, *Geophys. Res. Lett.*, **16**, 1067–1070.

Vaughan, P.J., Kohlstedt, D.J. & Waff, H.S., 1982. Distribution of the glass phase in hot-pressed, olivine-basalt aggregates: an electron microscope study, *Contrib. Mineral. Petrol.*, **81**, 253–261.